

Performance Index of a Network of Ground-Based Optical Sensors for Space Objects Observation and Measurements

Alessandro Urru

Michele Spanu

Enrico Congiu

Alessandro Palmas

Pietro Andronico

ITALY

alessandro.urrus@nurjanatech.com

ABSTRACT

The total number of space objects in Earth orbits is estimated to be over 200k, while the current number of those that are constantly tracked and cataloged is around 20k. In our era, where the space traffic is increasing every year, and so the risk of possible collisions, there is a global need to take control of the near Earth space environment, in particular the Low Earth Orbit. This is a common problem for every NATO country and it can be solved with a global collaboration between nations. In addition, the uncertainty associated with the measured position of orbiting objects is one of the main factors impacting performance, accuracy and timeliness. For this reason, aiming for the coordination of a multitude of sensors is one of the most important aspects targeted in the domain. This paper proposes an algorithm to estimate the performance of a globally-distributed network of optical assets (telescope and detector), with off-the-shelf telescope components, deployed in multiple sites distributed across different locations. In the context of space objects detection of size down to 3 cm, the quantitative performance measure is calculated as the portion of total cataloged debris that is visible by the network in a given time window (in our case, 24hrs have been considered). The proposed algorithm takes as input all the NORAD catalog, all the object physical data given by the DISCOS catalog, and all the optical and atmospheric data. It then propagates the space object population to obtain their position in the selected time window, filters out all the objects that are not in the ground station network line-of-sight for a sufficient amount of time to guarantee a feasible orbit determination, and on the objects satisfying all previous conditions it estimates the Signal-to-Noise Ratio achievable by the optical assets. These values are directly translated into a Probability of Detection, thus providing a performance index for the given Ground Sensor Network configuration that can be used as an objective function to be optimized when evaluating different architectures.

1.0 INTRODUCTION

In recent years, a new space-race has been happening. This is due to the fact that space is an incredible source of resources and useful data. This will translate into a rapid increase of satellites put into orbit around the Earth every year, and in particular in the Low Earth Orbit zone. More satellites means more possibility of collisions and disasters for the orbit environment as the famous Cosmos and Iridium collision in 2009 which generated thousands of new space debris. A recent report of ESA [1] has estimated the presence of 670k objects above 1 cm, and more than 1 million over 1 mm. One of the main problems is that one does not have full control over the orbital environment, and most of these objects are not cataloged or observed. The position measurements for a given satellite are usually not available in real-time, in fact they depend on its visibility from the selected sensor as well as sensor's accuracy, both factors directly impacting accuracy and precision of satellite orbital predictions. The development of a distributed sensor network, shared among NATO countries, would be a major improvement in this regard, allowing better monitoring of objects orbiting around the Earth.

An ideal network would be made of several sensors, insensitive to any atmospheric or astronomical perturbation, such as synthetic aperture radars. Unfortunately, such radars are expensive, difficult to

maintain, their installation requires several government permits and operations have to be supervised by highly trained personnel. Optical technologies, although limited by weather conditions and illumination, are a cheaper solution to deploy and to maintain. For this reason the study will focus on the implementation of an algorithm to find the best placement of a number of telescopes (with the same characteristics) given a list of possible sites (in the entire globe) and will provide as output the performance measure of this global optical network. The study is structured in six sections which describe: the algorithm structure, the general optical and astrodynamics theory behind the algorithm and two scenarios under study. The difference between the scenarios are only the number of possible telescopes to place for the calculations and each scenario has two possible optical configurations. The calculations are done with more than 12k cataloged objects from NORAD catalog with known physical characteristics (mainly size) and the analysis is done considering the performance mean values over a week of 24h propagations. At the end of the document conclusions of this study are presented together with possible improvements for the future works.

2.0 PROBLEM FORMULATION AND SOLUTION ALGORITHM

The goal of the algorithm developed for this study is to find the best placement of a number of telescopes for a global optical network, in terms of known LEO objects coverage as a function of a list of possible sites and a number of deployable sensors with the same characteristics. Each sensor will have a 24 hours observation interval and at least three acquisitions of the object can be taken (considering the sensor opening time) at least 10 degrees apart one from the other, from at least one sensor of the network. The object magnitude will be estimated and included in the visibility condition verification from the ground station. The key goal of this condition is to guarantee that orbit determination can be performed with the data acquired in the observation interval. This approach will allow to find the optimal trade-off between the number of deployed sensors and the reachable satellite population coverage.

The algorithm is structured in two main sections:

- *All sites visibility calculations:* For all the ground-station sites and using the optical asset configuration selected, the algorithm calculates the geometrical and optical visibility for all the 12K objects of the catalog. How the geometrical and optical visibility are evaluated is described below;
- *Find Best configuration:* Section that uses the data inside the visibility information calculated in All sites visibility calculations and a given number of the ground station available to find the best possible locations, considering all the possible combinations. This section is independent of other sections of the algorithm.

A summary of the algorithm structure is shown in figure 2-1.

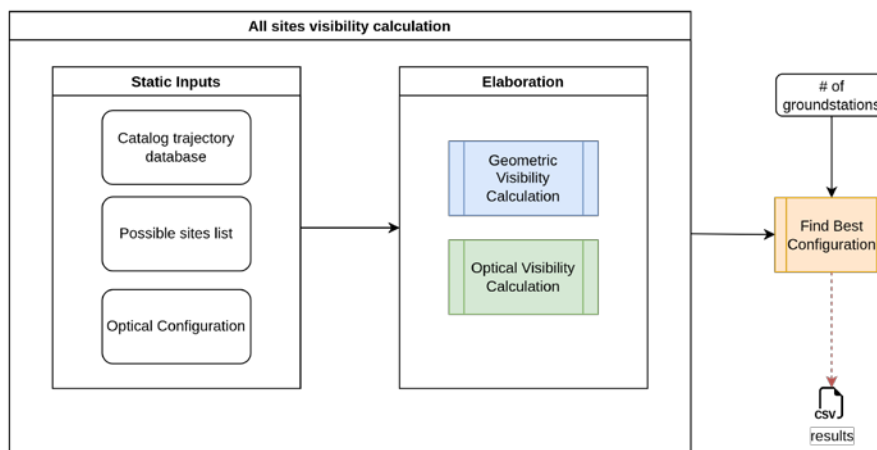


Figure 2-1: General structure of the algorithm.

Geometric Visibility is achieved if the following conditions are met:

- The satellite and the ground station are in Light of Sight (LOS) condition
- The elevation angle of the ground station to see the satellite is greater than a certain value (in this case 30 [deg]);
- The satellite is in LOS with the Sun and the ground station is in penumbra condition;
- The satellite trajectory, to be usable by a Orbit Determination Algorithm, must have an arch longer than a certain value (in this case three sensor acquisitions separated by 10 [deg] each).

All the objects having these characteristics are considered geometrically visible. Optical Visibility is computed only for the objects which are geometrically visible and is expressed by the target Detection Probability, based on the Signal Noise Ratio (SNR). The Detection Probability is the key parameter to evaluate the performance of the entire optical configuration and its computation is affected by the object passing multiple times over a certain position and by the object being seen from multiple locations.

This section takes as input:

- All the satellite catalog and its propagations (Catalog Trajectory Database);
- All the ground-station positions in WGS84 (latitude,longitude,altitude) and also their magnitude at zenith taken from [2];
- Detector parameters : pixel pitch, resolution in pixel, quantum efficiency, detector readout-noise, dark noise, binning mode;
- Telescope parameters: f# (f number), aperture diameter, optical transmittance, obscuration percentage.

3.0 ASTRODYNAMICS AND OPTICAL THEORY

As described before the study aims to solve both astrodynamics and optical equations.. The description of both theories is the following.

3.1 Astrodynamics Analysis

The astrodynamics analysis starts from the computation of the satellites' trajectories in Earth orbit using the 18th Squadron Elsets. Using the computed trajectories and the ground station positions, the celestial trajectories in terms of Azimuth, Elevation and Range are computed with respect to each station local frame. However, since we are dealing with optical sensors, satellite visibility from a ground station requires certain conditions to be met, such as: line of sight between satellite and the ground sensor, satellite illuminated by the sun and ground station in the darkness. To do so, the visibility windows computations are performed by three main software modules described in figure 3-1.

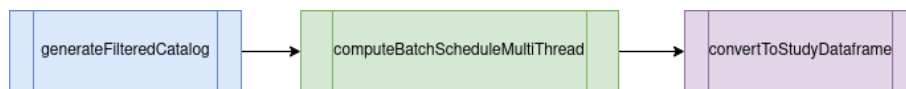


Figure 3-1 : Computation steps to perform visibility windows diagram

- *generateFilteredCatalog*: computes the trajectories of the selected satellites batch. Satellites are filtered based on orbit altitude and physical size. An approximate batch size is around 10k satellites;

- *computeBatchScheduleMultiThread*: computes the visibility windows using stations parameters (latitude, longitude, altitude, type) and windows constraints (elevation threshold, arc length threshold) for each station available on database;
- *convertToStudyDataframe*: converts the processed data in a format suitable for the optical performance algorithms. This is a data reduction process which keeps only the metrics relevant for the study.

Results are then stored in a dataframe of observation windows containing the following data:

NORAD ID	Passage ID	Elevation angle	Distance	Phase angle	Object diameter
----------	------------	-----------------	----------	-------------	-----------------

These data will serve as input for the optical performance evaluation.

3.2 Optical Analysis

3.2.1 From Signal To Probability Detection

To obtain the probability detection is necessary to obtain the signal-to-noise-ratio of the system. Which is defined as [3]:

$$SNR = \frac{S}{\sqrt{S + BG + RN^2 + DN^2}}$$

Where S is the target signal component [photoelectrons], BG is the background component [photoelectrons], RN is the detector read noise component [photoelectrons^{1/2}] and DN is the detector dark current component [photoelectrons^{1/2}]. The procedure to convert the apparent magnitude signal into photoelectrons is described in [2] as :

$$S = QE \cdot \tau_{lens} \cdot A \cdot E_{target} \cdot t_{int} \cdot \tau_{atm}$$

Where S is the apparent magnitude signal [photoelectrons], QE is the detector quantum efficiency, τ_{lens} is the lens transmittance, A is the optical aperture area [m²], E_{target} is the photon flux density from the target [ph/sec/m²], t_{int} is the integration time [sec]. The τ_{atm} is the atmospheric transmittance and is expressed by:

$$\tau_{atm} = \tau_{atm0}^{\sec(\pi/2-\phi)}$$

Where τ_{atm0} is the atmospheric transmittance at the zenith as altitude dependent, described in 3.1.2 paragraph and ϕ : telescope elevation angle [deg]. A deeper consideration about the integration time must be done. The integration time is obtained by summing the exposure time and the detector reading time (valid only if the target is still in front of the lens/detector). In this particular scenario the target is not still in the pixel but it will stay inside it for a very limited amount of time. To obtain a good estimate of the signal-to-noise ratio, in this case it is necessary to consider the integration time as the time spent by the target in a single pixel. Assuming a gaussian distribution, the probability detection can be obtained as [5]:

$$P_d = \sqrt{\frac{1}{2\pi}} \cdot \int_0^{SNR} e^{-0.5 \cdot (s-3)^2} ds$$

The algorithm takes in account also if a satellite has multiple passages in the same or in more ground station sites and of course this affects the probability detection of the single satellite in the optical network. This is

possible considering a passage, a probability of an independent event and merging all the probabilities using the 'at least once' rule.

3.2.2 Atmospheric Transmittance

To evaluate the accurate impact of the atmosphere on optical performance, altitude-dependent atmospheric transmittance modeling was developed. To find the equation that simulates the behavior of altitude observer-dependent zenith transmittance, studies reported in [3] were tested. Taking into consideration a specific wavelength-dependent atmospheric transmittance from MODTRAN, we derived the fitting equation by varying the altitude. The simulation of the curves in [4] was implemented using MODTRAN.

3.2.3 Chosen Configurations Characteristics

To achieve these performances in terms of minimum satellite size it is crucial to choose the right optical asset to be sure to detect the majority of cataloged objects and, last but not least, this asset must be physically realistic. To detect small objects (< 15 cm) it is necessary to use telescopes with a large aperture (> 400 mm). These kinds of telescopes have a very high fixed focal length (> 1000 mm). The aperture and focal length are related parameters: high aperture means a high focal length. This is an important aspect to evaluate because it is a physical limit for our use case. Acquiring measurements with bigger aperture optics means that the received signal is stronger but with a very narrow Instantaneous Field Of View (IFOV) which will translate in a very short elapsed time of the target in the pixel and so into an exponential decrease of the signal and the probability detection. To evaluate the performance of each configuration, the probability detection has been calculated, related to the following conditions:

- Elevation angle from 30 to 90 [deg];
- Target altitude from 200 to 2000 [km];
- Phase angle of 30 [deg];

Starting from these conditions, two different optical configurations were chosen. A summary of their parameters are listed in Table 3-1.

Table 3-1: Parameters of two optical assets.

Parameter	Configuration 1	Configuration 2
Primary Mirror Diameter [mm]	800	400
Focal length [mm]	3040	1520
Focal Ratio	3.8	
Linear Obstruction [%]	55	
Pixel Resolution	6144x6144	4096x4096
Pixel Size [μm]	10	9
Read Out noise [e-]	4.2	3.7
Dark Current [e-/s]	0.07	0.15
QE [%]	70	70

Evaluating the proposed scenario with these 2 telescopes configurations, the achieved results in terms of probability detection (greater than or equal to 20%) are listed in Table 3-2.

Table 3-2: Detection Performances of Optical Assets.

Object Size [cm]	Configuration 1	Configuration 2
	Reached Altitude [km]	
10	> 2000	> 2000
5	> 2000	~ 1600
3	~ 1200	~ 500

4.0 SIMULATIONS AND RESULTS

In order to define the performance of the network, two scenario simulations were performed. For the first one, it was assumed to have ten different sites to make observations and for the second scenario, twenty-one different sites. It is important to emphasize that every selected location is an existing ground station, excluding the Sardinia site. The locations are chosen among the best zenith sky magnitude levels. The simulations were performed considering a filtered Norad catalog, where objects meet the following constraints:

- The objects must be under 2000 km;
- The catalog propagations computed on 24h observational window;
- Three acquisitions of the object can be taken (considering the sensor opening time) at least;
- An angular distance of 10 degrees apart one from the object to another, from at least one sensor of the network;
- Only objects with known sizes are considered. To obtain these data it has been used the SATCAT catalog (Celstrack).

The assumptions made for the algorithm were as follows:

- The object will be always centered in the FOV and assumed as spherical;
- Clear sky visibility (> 50km) and a very dark background (> 20 mag);
- Telescope Elevation > 30°.

To obtain a more accurate representation of the network performance, a weekly temporal mean of the algorithm results was performed, considering that each day has its own results. Observation window from 29/05/2022 to 05/06/2022 was taken into account for simulations.

The considered possible sites are in Table 4-1.

Table 4-1: Possible selected sites.

Observatory Tag	Country Republic of South Africa	Latitude [deg]	Longitude [deg]	Altitude [m]	Zenith Magnitude [mag./arcsec ²]
<i>grst_1_ITA</i>	Italy	39.60005	9.63934	330	21.87
<i>grst_2_CHI</i>	Chile	-24.6274	-70.4038	2635	22
<i>grst_3_USA</i>	USA	32.7805	-105.821	2788	21.87
<i>grst_4_SPA</i>	Spain	28.75659	-17.8919	2252	21.92
<i>grst_5_FRA</i>	France	42.93655	0.1423	2870	21.73
<i>grst_6_GER</i>	Germany	47.70404	12.0133	1838	21.62
<i>grst_7_USA</i>	Hawaii	19.82562	-155.472	4205	21.98
<i>grst_8_CAN</i>	Canada	45.4549	-71.1533	1111	21.9
<i>grst_9_SPA</i>	Spain	28.75399	-17.8891	2387	21.92
<i>grst_10_BUL</i>	Bulgaria	41.69312	24.73782	1735	21.85
<i>grst_11_AUS</i>	Australia	-31.2755	149.0672	1165	22
<i>grst_12_RSA</i>	Rep. of South Africa	-32.3756	20.8108	1798	22

<i>grst_13_IND</i>	India	12.57628	78.8263	700	21.82
<i>grst_14_IND</i>	India	32.77955	78.96383	4500	22
<i>grst_15_IDN</i>	Indonesia	-6.82621	107.607	1280	20.41
<i>grst_16_NOR</i>	Norway	69.58649	19.22586	70	20.77
<i>grst_17_NZL</i>	New Zealand	-43.9874	170.4641	1017	21.97
<i>grst_18_MON</i>	Mongolia	51.61983	100.9214	1994	22
<i>grst_19_IRL</i>	Ireland	53.91464	-8.37035	86	21.79
<i>grst_20_DEN</i>	Denmark	55.62195	11.68131	59	21.47
<i>grst_21_NAM</i>	Namibia	-23.2339	16.36882	1834	22

To understand how the optical network performance changes with the choice of the possible places, two different scenarios were taken into account: Scenario 1 that includes the first 10 sites listed in Table 4-1 and Scenario 2 with all the sites listed in Table 4-1.

For each scenario, the number of the available telescopes to be placed goes from 1 to the maximum number of available sites. For each site, the same telescope configuration was assumed. The locations are shown in figure 4-1.



Figure 4-1: Map of the observatory sites taken into account for the study. The highlighted points are related to scenario 1 and include the first ten positions of Table 4-1.

The performance of the single site is expressed in Figure 4-2. It can be noted that some positions are way more efficient than others, this depends by the latitudes and by the period of the year evaluated for the simulation which affects the elevation angle of observation and so the atmospheric transmittance (some latitudes can give better angles than others for LEO objects). It is also worth noticing that if a station sees a lower percentage of the catalog it can see objects completely different from a station with a higher percentage so in a configuration they could compensate for each other and the algorithm takes this into account. Last but not least, it should be noted that one station is not giving any results and has 0% of coverage, the station is the one in Norway. This is because during the simulation period this station is

constantly under the sunlight for the particular conditions of these high latitudes. So this is another aspect that the algorithm takes into consideration during the performance evaluation of the entire network.

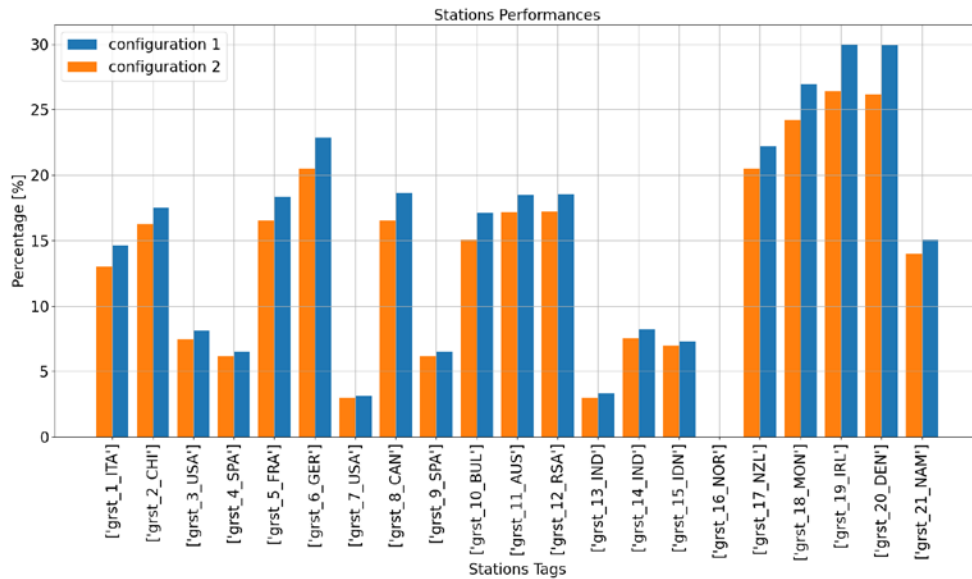


Figure 4-2: Percentage of NORAD catalog visibility for every ground station.

4.1 Scenario 1

In this case, the percentage of detected objects dependent by size range for both optical configurations is shown in figure 4-3. As can be seen, most objects result in the range of 5-10 [cm] with approximately 20% of detected objects. For smaller objects under 5 cm, the value drops below 3% for the configuration 1. This is due to poor knowledge of small satellites in LEO orbit in NORAD catalog.

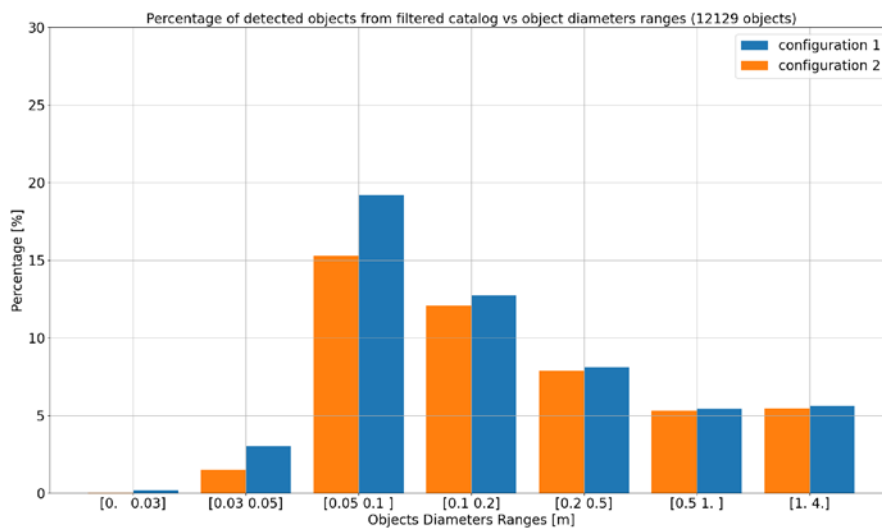


Figure 4-3: Comparison of detected (with a probability detection threshold > 20%) objects with the two optical configurations for scenario 1.

Figure 4-4 shows the results of the ground stations combination performances. After using 5 ground stations

simultaneously, the percentage stays constant around 54%.

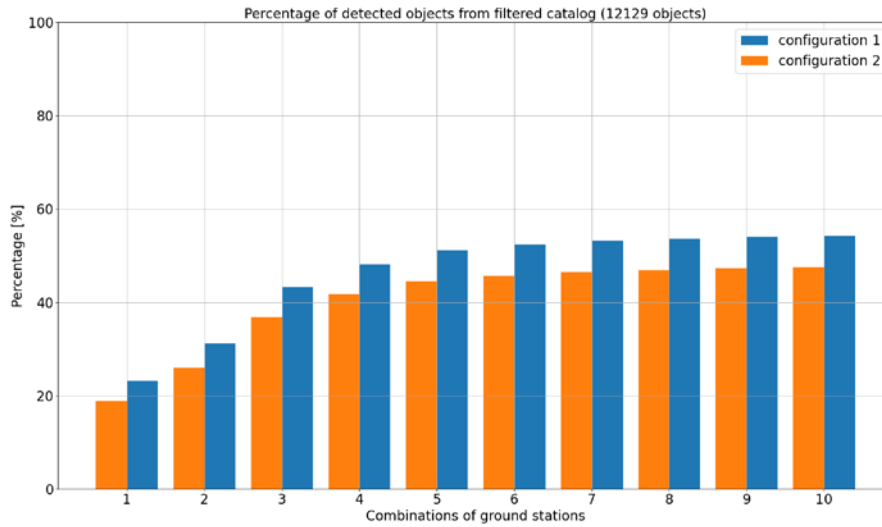


Figure 4-4: Percentage of objects detected combining the ground stations performances based on input NORAD catalog filtered for scenario 1.

Figure 4-5 shows the probability distribution of space debris in LEO for configuration 1. As can be seen, a massive concentration of small elements in the 600-800 km layer with a very low detection rate. The huge difference between this layer and the upper layers is due to the extreme velocity of the objects of about 7.5 km/s [6].

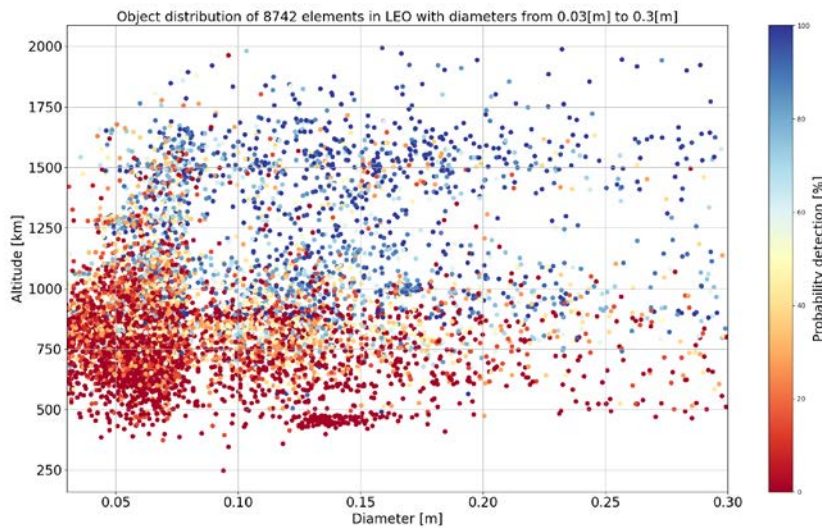


Figure 4-5: Percentage of objects detected combining the ground stations performances based on input NORAD catalog filtered for scenario 1.

4.2 Scenario 2

In this scenario, new stations were added with respect to the previous one distributing them on a broader range in terms of latitude. The new stations have a better coverage of the target objects with respect to the previous case. As figure 4-2 shows, the ground stations with highest visibility (more than 20%) are around the same latitude. In particular, it can be seen that *grst_16_NOR* in Norway for this test time window, has

zero visibility and therefore won't play a role in this specific simulation. This is due to the fact that the considered time windows are in spring/summer when, in higher latitude countries, the light period is so long that visibility to the optical telescope is not guaranteed. In figure 4-6 the percentage of detected objects as a function of the size for both optical configurations is shown. Compared with the results described in 4.1 section, an overall increase in detection probability can be seen for all object sizes. The most relevant results are seen for the smallest objects: with configuration 1, objects under 5 cm can be detected. This opens a new window to catalog a new set of micro space debris that turn out to be the most dangerous in LEO orbit.

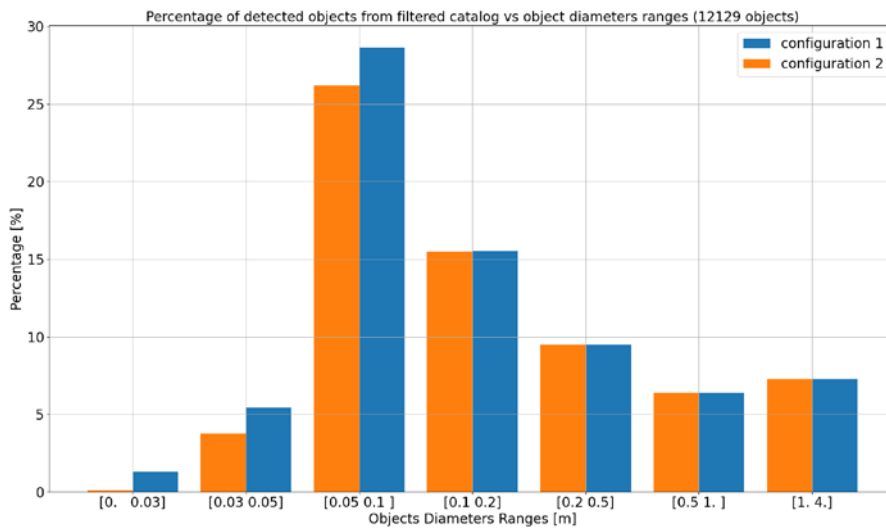


Figure 4-6: Comparison of detected (with a probability detection threshold > 20%) objects with the two optical configurations for scenario 2.

As shown in figure 4-7 after using 5 ground stations simultaneously, the percentage is more than the use of all stations considered for scenario 1 and after using 10 ground stations, the percentage stays constant around 74% (20% more with respect to scenario 1 performances).

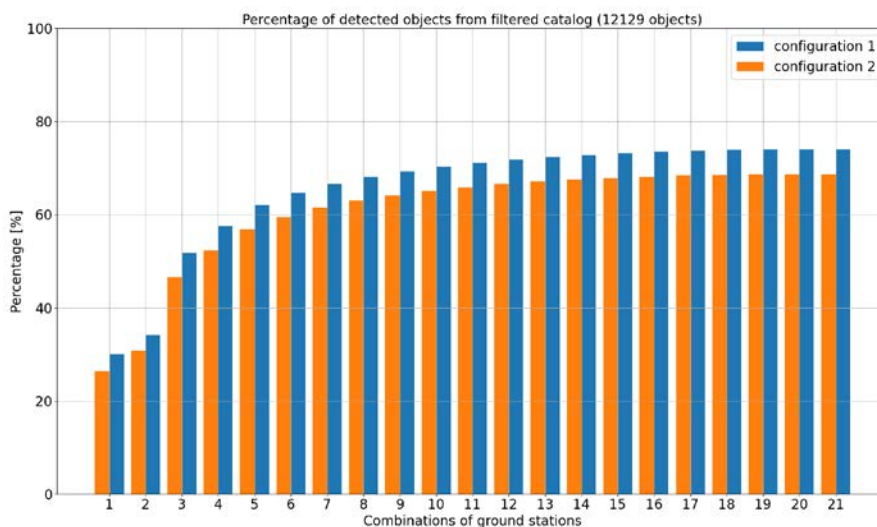


Figure 4-7: Percentage of objects detected combining the ground stations performances based on input NORAD catalog filtered for scenario 2.

Figure 4-8 shows the probability distribution of space debris in LEO for configuration 1. Comparing this

result with the one previous scenario, there is a significant improvement. Despite a considerable number of elements with low values of probability, the mean value of probability of detection increases around 70%.

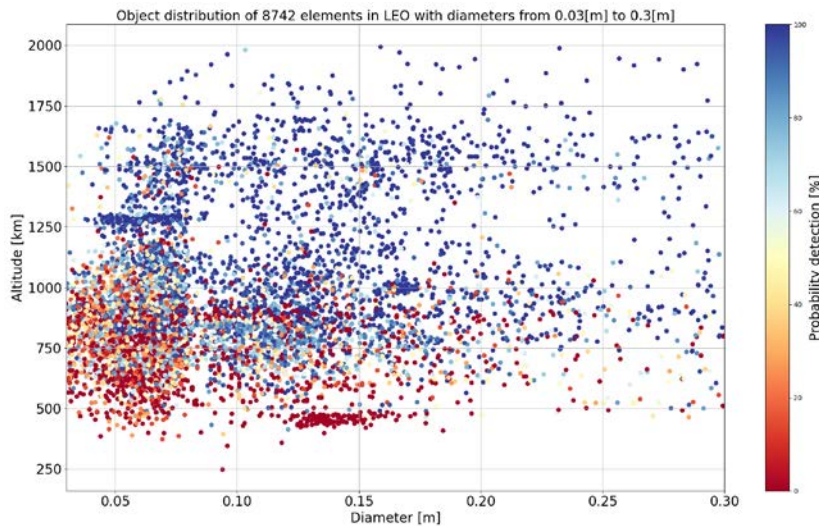


Figure 4-8: Distribution of satellites in LEO according to their diameter and altitude values for Configuration 1 for scenario 2.

5.0 CONCLUSIONS

Space objects monitoring, in recent years, has become a challenge both to have a clearer picture of the space environment around the Earth and to perform more precise maneuvers to avoid possible collisions, especially for the increasing number of companies that are investing in the launch of space assets.

Most of these objects are resident in LEO orbit and many of them, due to small size (<15 cm) are untracked nowadays. The aim of this paper was to develop a practical tool which allows to easily design and evaluate the performances of an optical telescope sensor network around the globe with the aim to maximize the satellite detection probability. In this paper two different simulation networks are evaluated: one with 10 sites and one with 21 sites. Analyzing and comparing the two different networks results has highlighted some practical rules to assure a good design of a telescope optical network. Spreading the network all over the world guarantees to cover as many different latitude locations and a better observation sky window. This is due to the possibility to have different elevation angles for each station for the same satellite, increasing the probability to have more passages near the zenith with a lower atmospheric attenuation. Under this condition, extreme latitudes can be useless in some periods of the year (due to the extreme long period of sun exposure). Therefore, it is crucial to evaluate this geographics limitation to place an optical telescope. As can be noticed in figure 4-7, a good choice of ground station sites is more impactful on the results than the actual number of ground stations chosen to maximize the number of satellites detected. A second consideration is about the type of the optics and detector choice. The choice of the components are crucial to reach the slightest light reflected by a satellite and so also the smaller debris < 5 cm can be theoretically seen in good weather conditions. Choosing a bigger telescope to detect very small objects does not necessarily translate into better results. In the hypothesis of a large aperture telescope and related narrow beam, the observation of LEO objects is not guaranteed due to extreme velocities of the objects that reduce the permanence time of it in the pixel and so a very low signal to the detector. In this case a smaller optical asset could be better than a bigger one.

This tool has been proven to have a great potential to calculate the performances of an optical telescope network. Different improvements could be adopted and will be subject of future work: it would be useful to

use additional data from different catalogs, in fact the statistical performance measure is highly affected by the objects considered, in this case those present in the Norad catalog (only the ones with known sizes). Also having better albedo measurements for the satellites would make the calculation more accurate. Another aspect to improve is the observation window length of the study, that could be increased from a week to a year to estimate better statistics.

6.0 REFERENCES

- [1] https://www.esa.int/Space_Safety/Clean_Space/How_many_space_debris_objects_are_currently_in_orbit
- [2] <https://www.lightpollutionmap.info/>
- [3] Gerald C. Holst (2017). Electro-Optical Imaging System Performance. JCD Publishing, SPIE.
- [4] James R. Shell (2010). Optimizing orbital debris monitoring with optical telescopes. US Air Force, Space Innovation and Development Center 24 Talon Way, Schriever AFB, CO 80912
- [5] William Wan (2009). Passive IR Sensor Performance Analysis using Mathcad® Modeling. Proc. SPIE 7300, Infrared Imaging Systems: Design, Analysis, Modeling, and Testing XX, 730005.
- [6] Roger R. Bate (1971). Fundamentals of Astrodynamics.